Nuclear Spectroscopy Group activities around MARA and RITU separators at JYFLACCLAB

NUSPRASEN Workshop 2019
GSI, Darmstadt

Content:

- Introduction
- MARA and RITU separators
- Some recent results
- Plans for the near and distant future

Juha Uusitalo
Nuclear Spectroscopy Group
Department of Physics
University of Jyväskylä (JYFL)
Finland

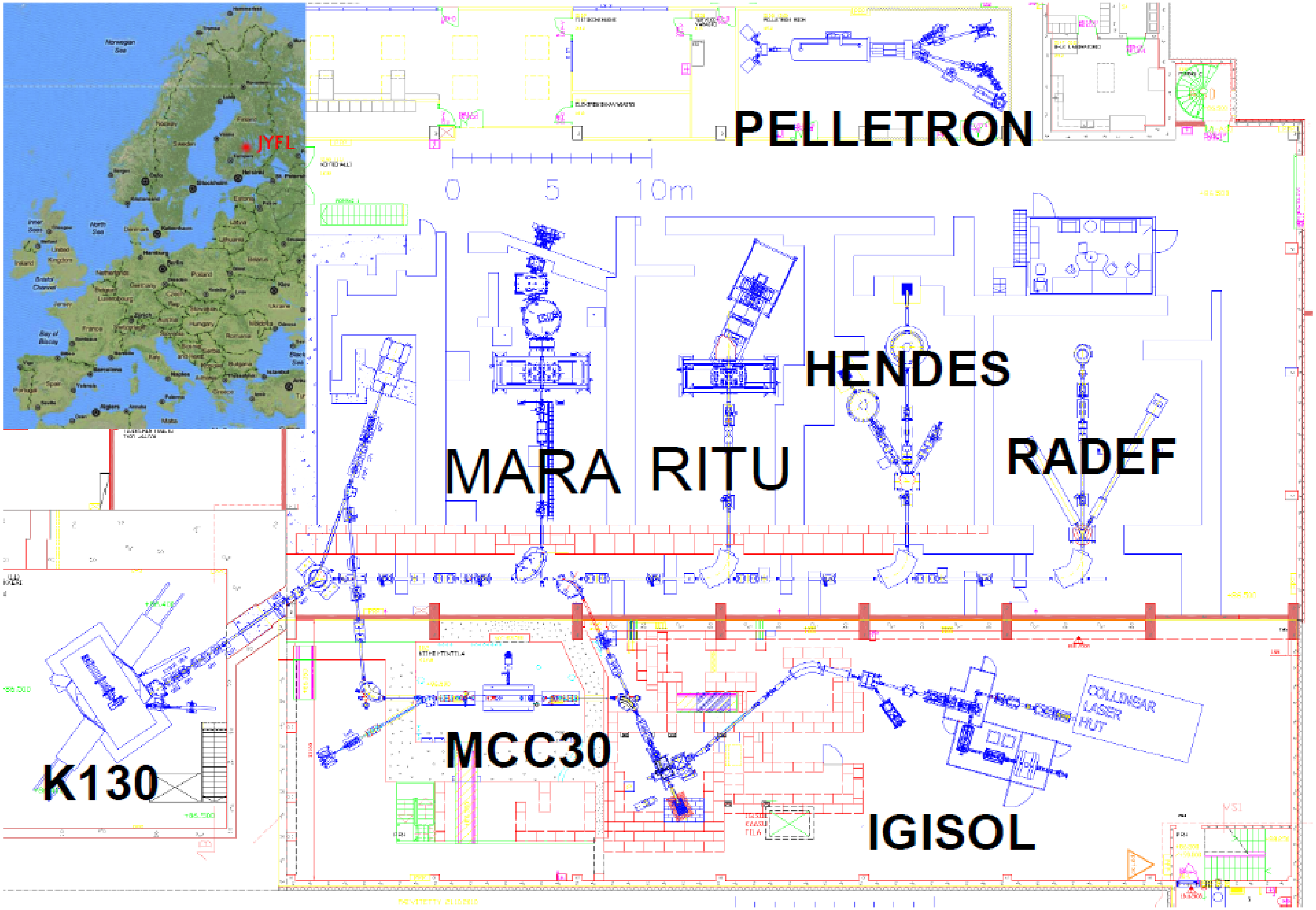
JYFL
0 5 10m
PELLETRON
HENDES
RADEF
MARA
RITU
MCC30
K130
IGISOL
COLLINEAR LASER HUT

RITU, Recoil Ion Transport Unit
In operation since 1994
In avg. > 10 ref. publications/y

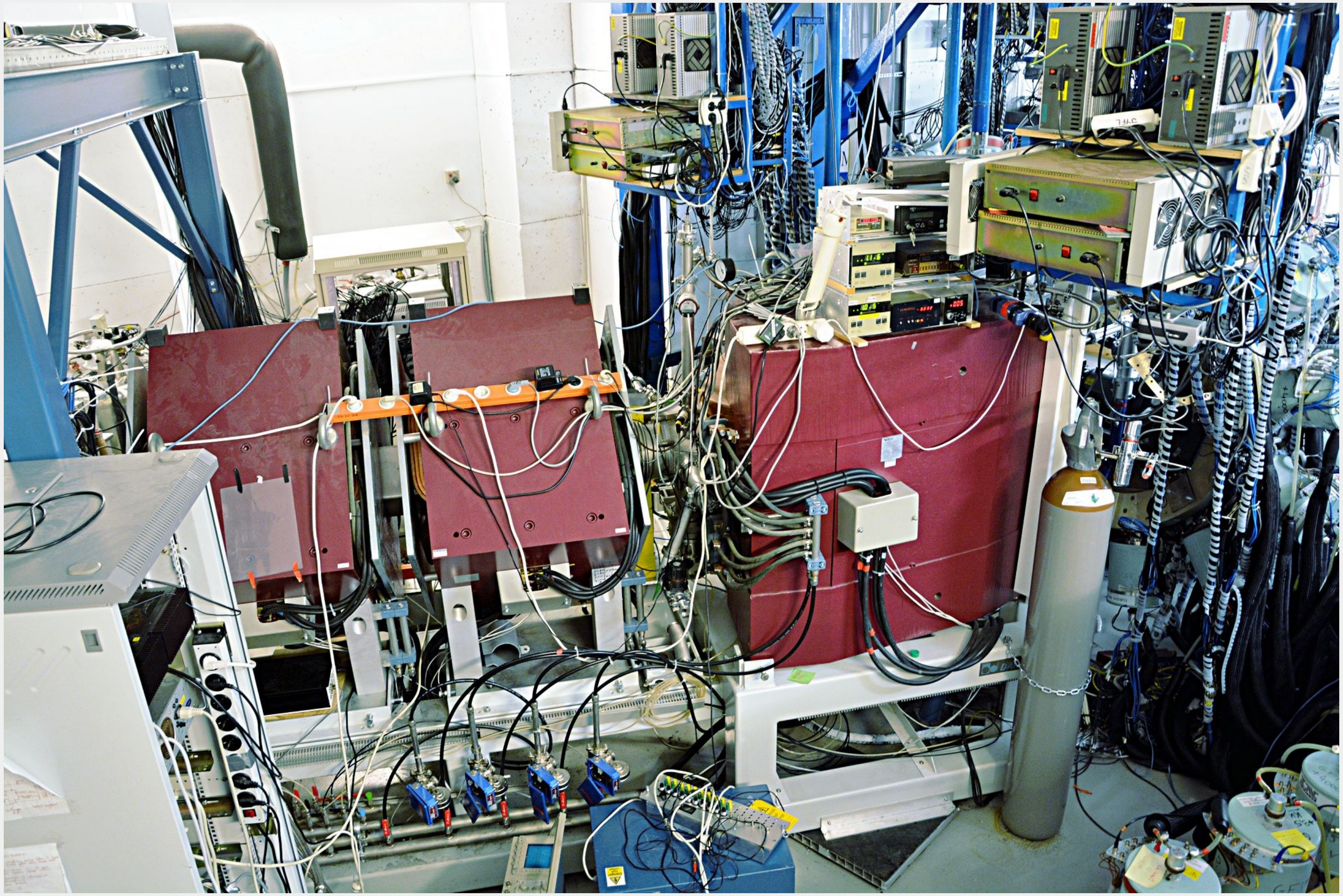

MARA – *M*ass *A*nalysing *R*ecoil *A*pparatus

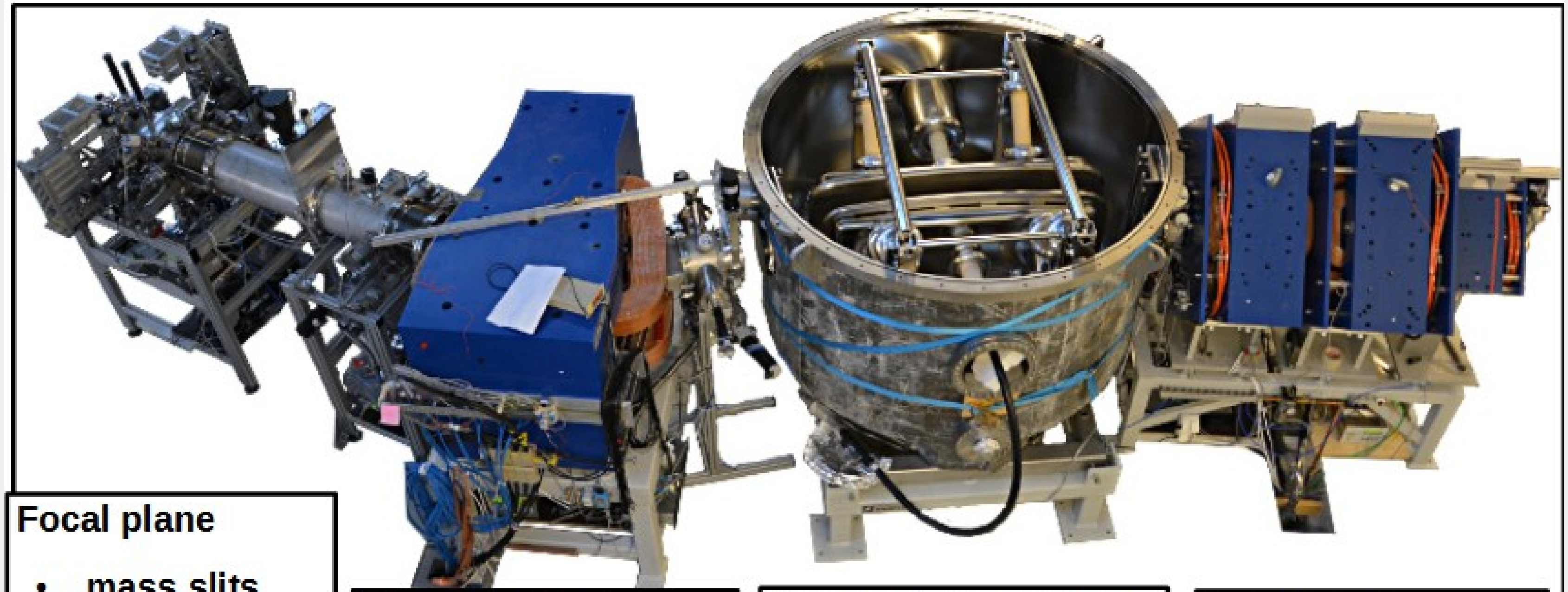

Focal plane

- mass slits
- MWPC, DSSD, Box detector and Ge array

Magnetic dipole

- 1 T, 1 m radius
- adjustable surface coils to change focal plane position

Electrostatic deflector

- beam separation
- +- 230 kV, 4 m radius
- split anode and a beam dump

Quadrupole triplet

- scalable first order resolving power

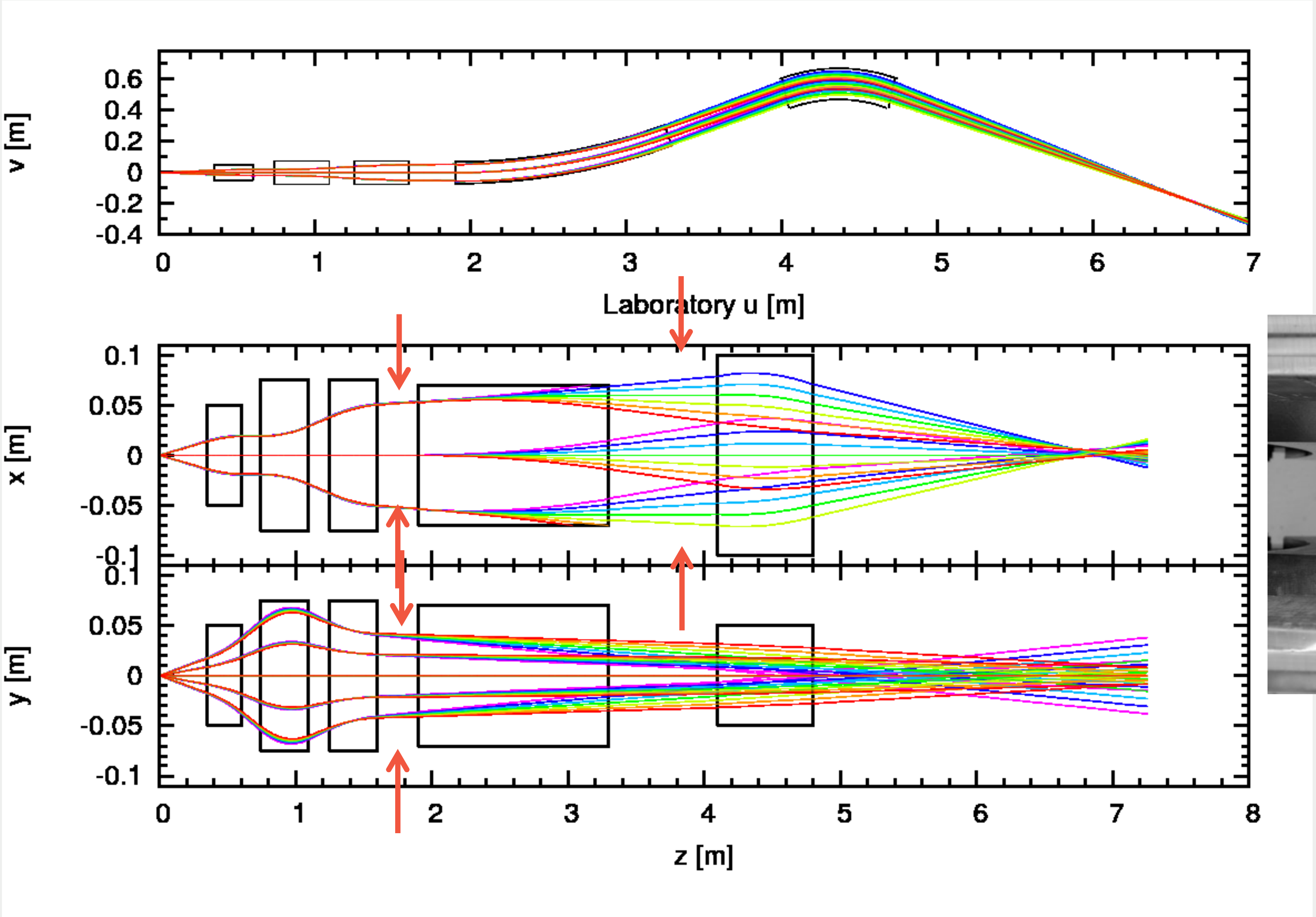

First order resolving power 259
Angular acceptance 10 msr
Energy acceptance – 15 % - + 20 %
Charge state acceptance ± 7 %
M/Q dispersion 8.1 mm/%

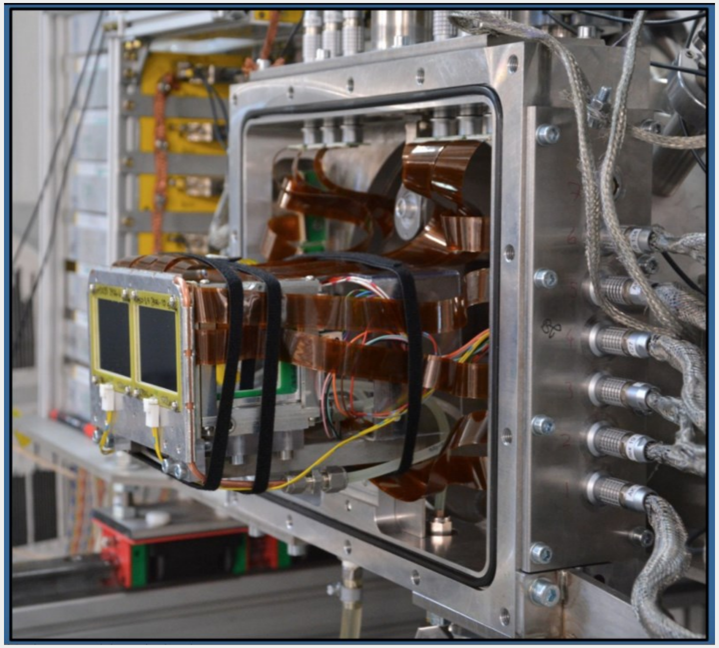

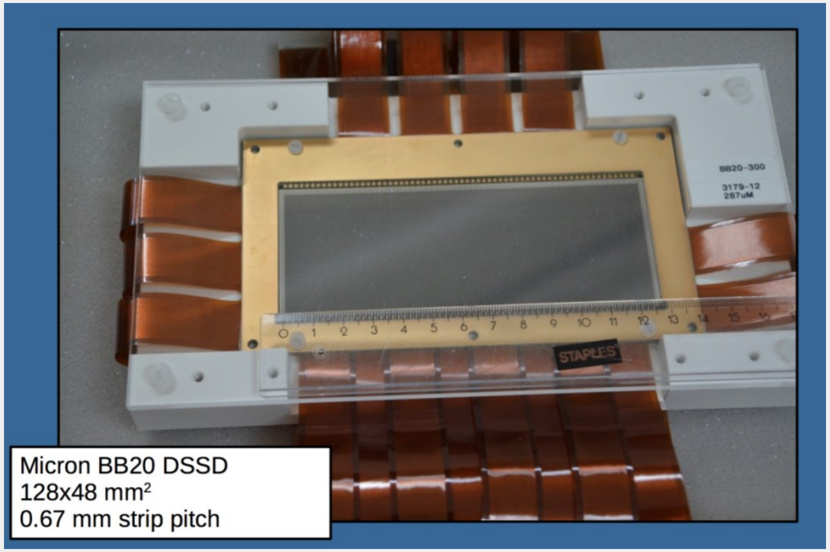

192x72=
13824
pixels

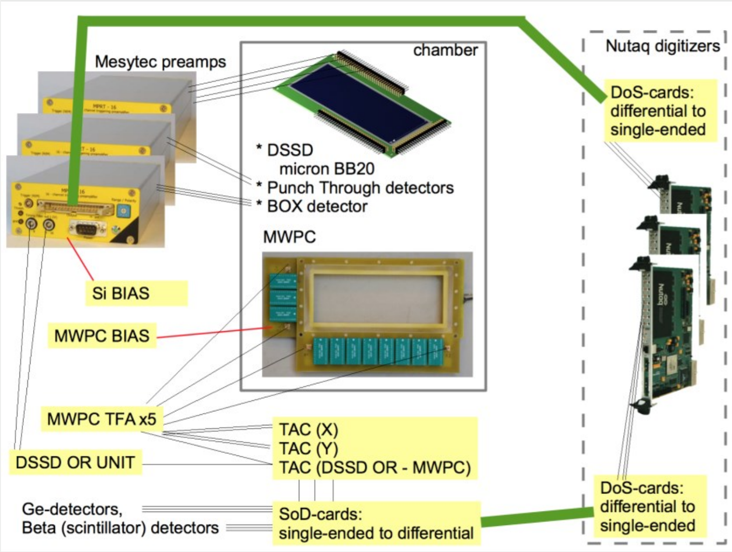

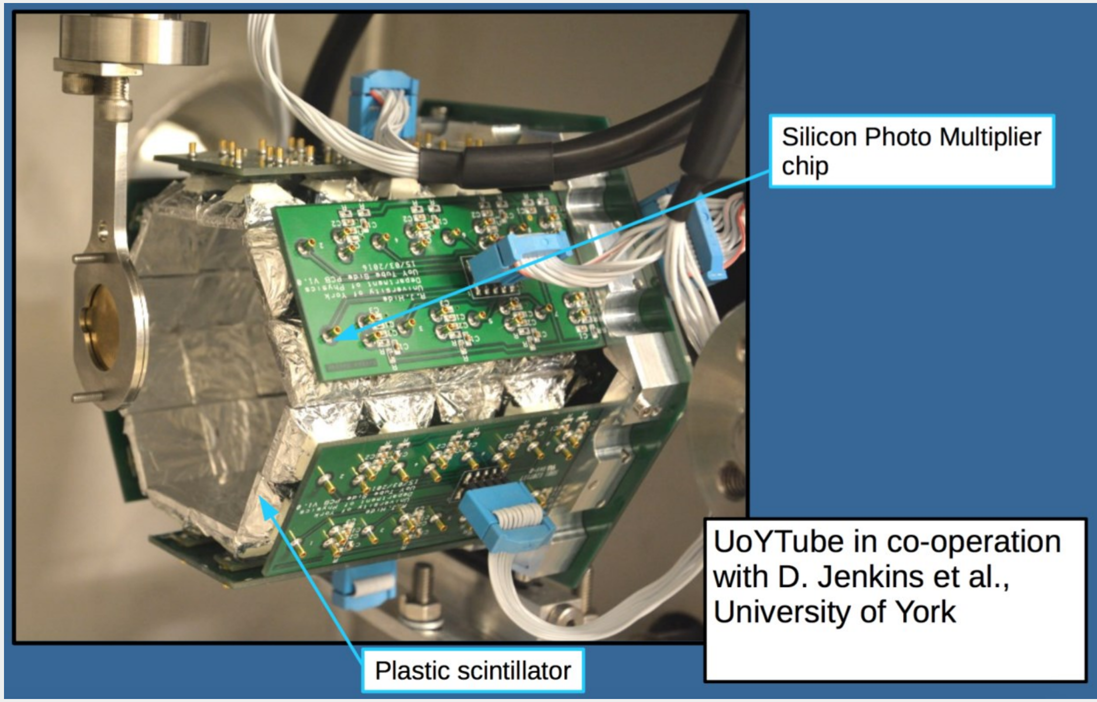

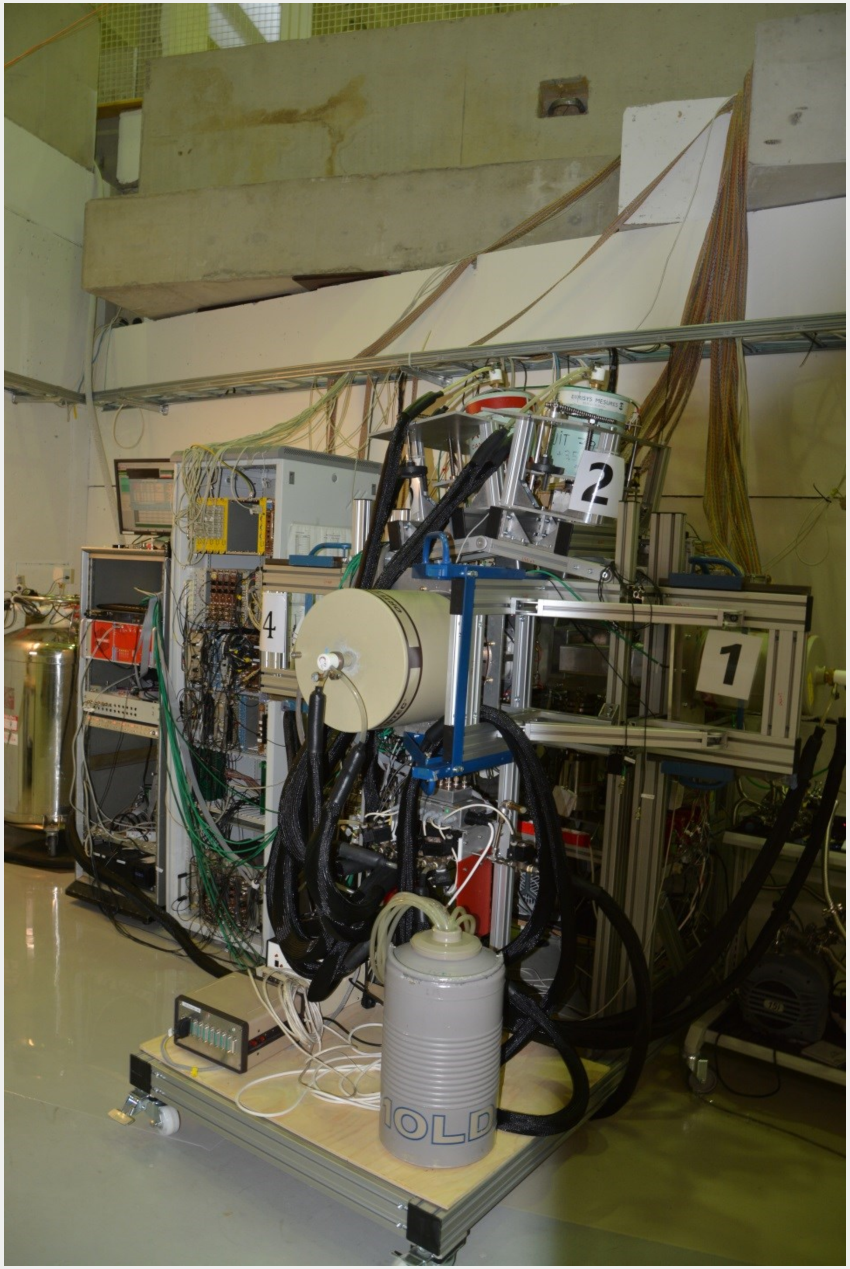

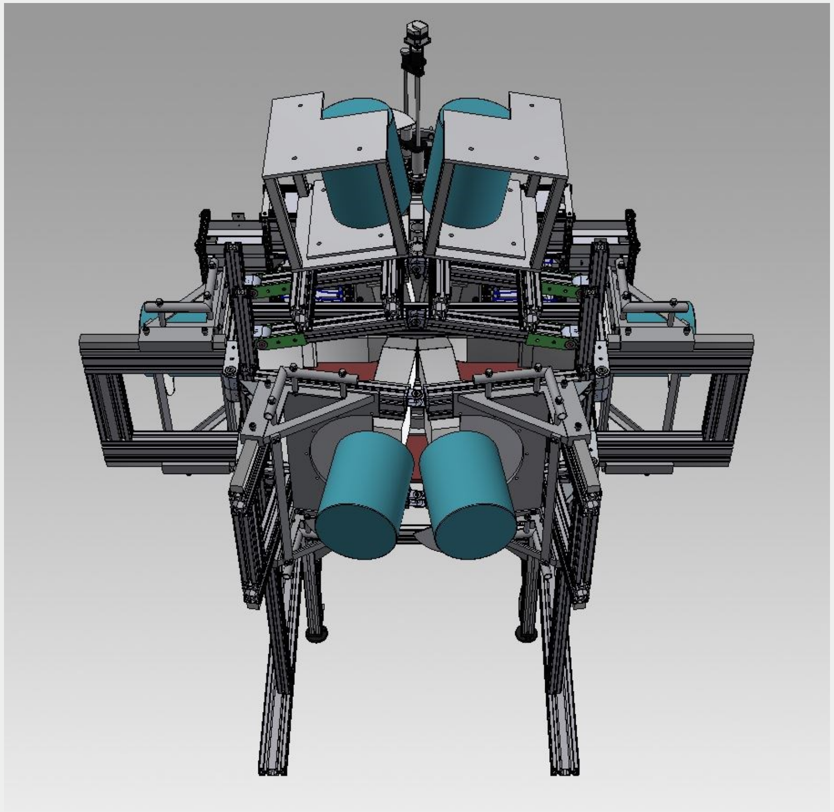

BGO-shields, University of York

2-3 BeGe detectors, FIRI-infra

Mass/charge ratio of fusion products
Example: reaction 58Ni + 106Cd → 164Os

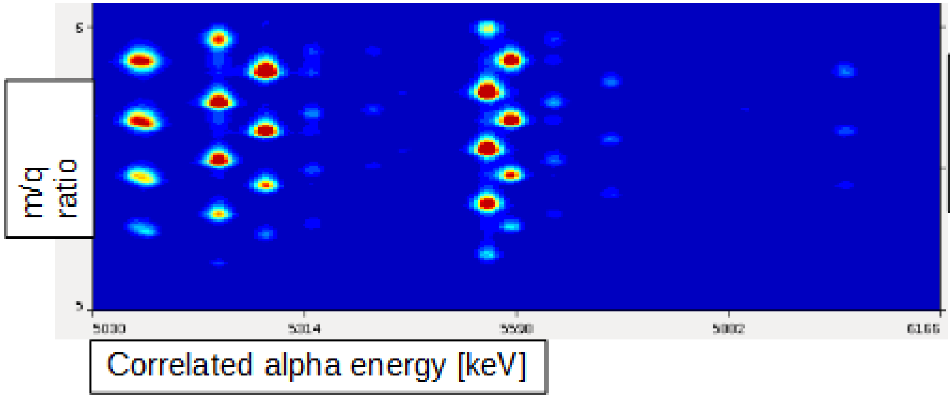

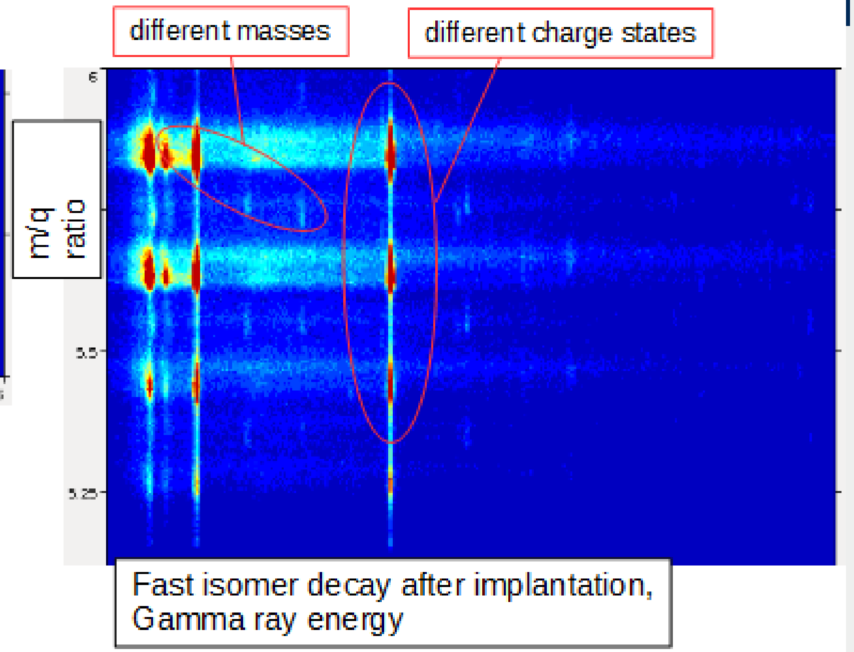

Isomeric gamma decay tagging selectivity can be enhanced by the mass resolving power.

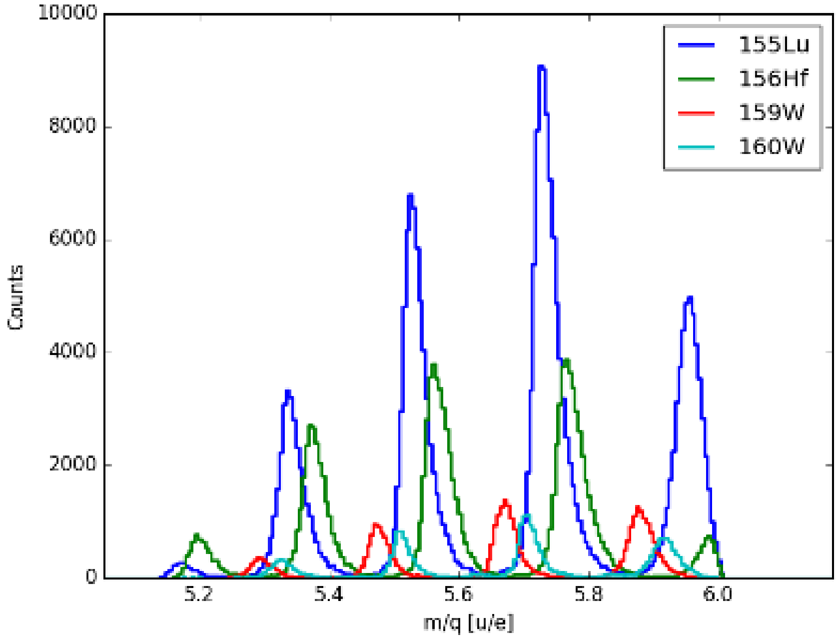

Mass resolving power of 140-150 was obtained in this reaction. It is strongly affected by beam spot size and aberrations. If required, mass resolving power can be increased by apertures or by using a so called high resolution mode.

JUROGAM3

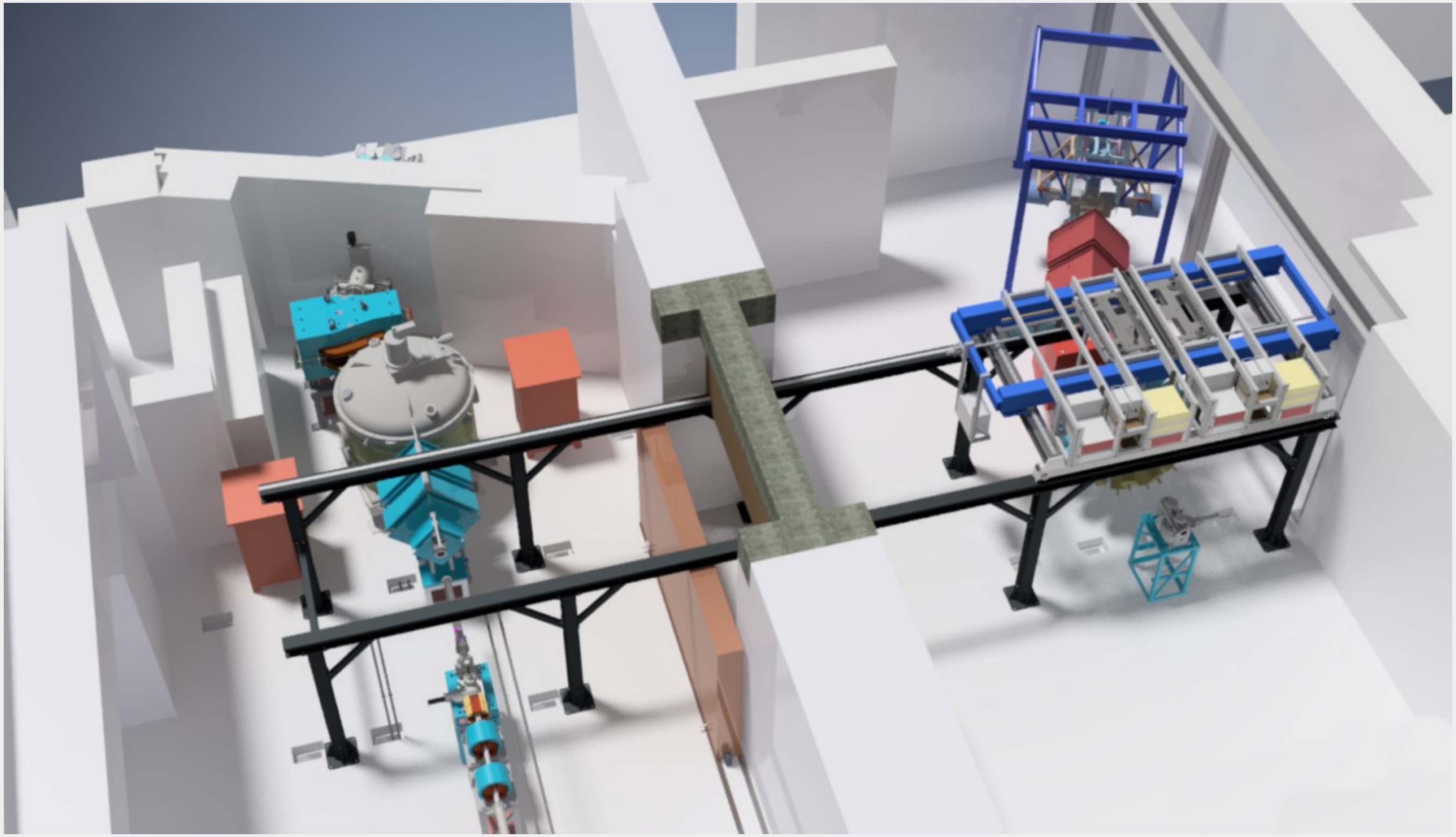

In-beam and delayed spectroscopic studies at N=Z line and beyond

DEPARTMENT OF PHYSICS
UNIVERSITY OF JYVÄSKYLÄ
RESEARCH REPORT No. 8/2013

Development of the recoil-beta tagging method and recoil-beta tagging studies of ^{66}As and ^{66}Se

by

Panu Ruotsalainen

Academic Dissertation
for the Degree of
Doctor of Philosophy

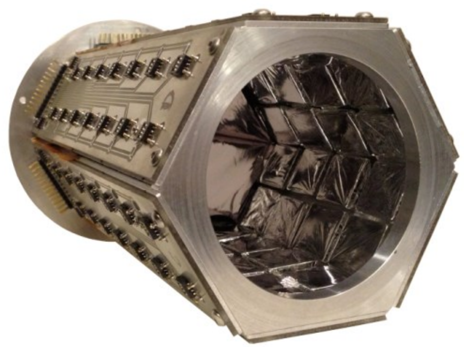

Figure 4.1: Photograph of the UoYtube charged particle veto box from beam direction. 96 CsI(Tl) crystals are arranged around the 6 sides of a hexagonal barrel. Each crystal is sealed within thin mylar foil and Ni foils with thickness of 2.5 μm were applied to all surfaces at forward angles covering the first four pairs of crystals.

Collaboration with the University of York, UK

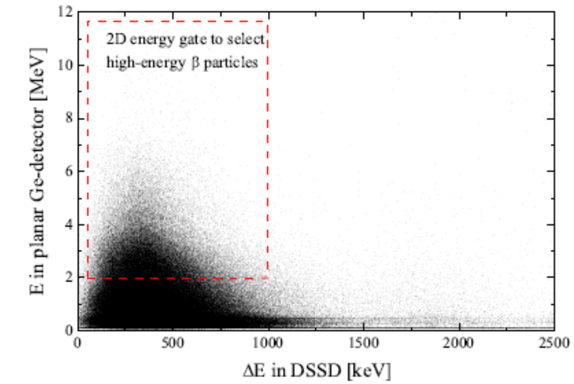

Figure 2.7: Identification matrix for high-energy β particles. The energy-loss information (ΔE) is obtained from the DSSD (x axis) and full energy information (E) from the planar germanium detector (y axis). A two-dimensional energy gate can be applied to select β particles to be correlated with recoils within a desired correlation time. The low-energy detection threshold can be varied in order to achieve better statistics or cleanliness of the tagged spectra.

CED Coulomb Energy Differencies, JM2,
- Z = N - 2 or Z = N + 2

MED Mirror Energy Differencies, M4, M11, JM2, JM8, JM11, JM12
- number of protons and neutron interchanged

TED Triplet Energy Differencies, JM2, JM4, JM7, JM10, JM13
- complete isobaric triplets
- T_z = (N-Z)/2 = 0, ±1

Isoscalar np-pairing and delayed alignment N = Z, JM5, JM9

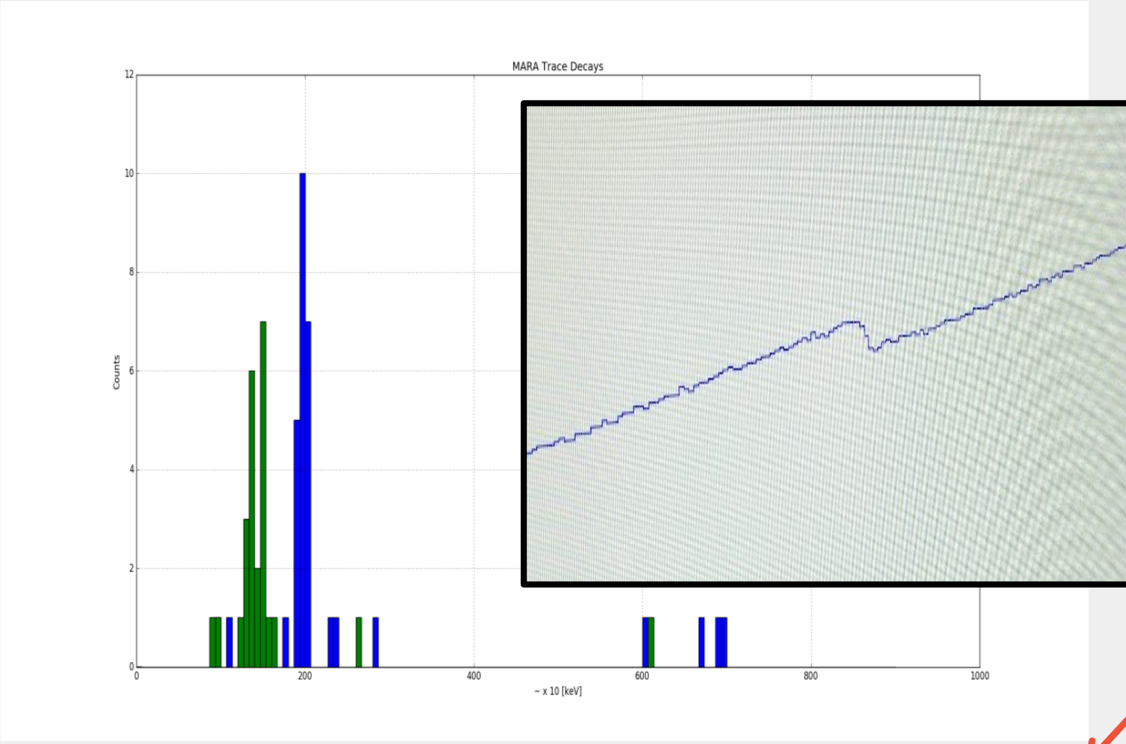

J. Hilton et. al., to be published

^{169}Au
^{168}Pt
^{165}Ir
^{164}Os
^{160}W
^{156}Hf

^{78}Kr + ^{96}Ru -> ^{174}Hg*
^{78}Kr + ^{92}Mo -> ^{170}Pt*

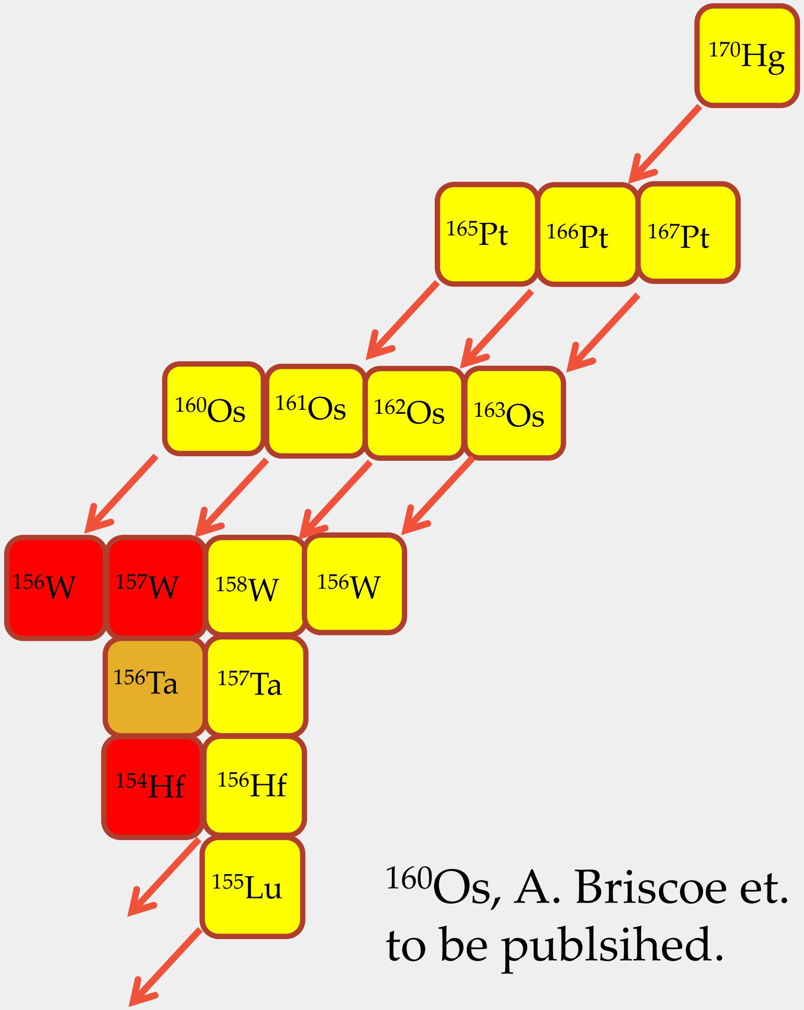

^{78}Kr + ^{96}Ru -> ^{174}Hg*
^{78}Kr + ^{92}Mo -> ^{170}Pt*
^{58}Ni + ^{106}Cd -> ^{164}Os*

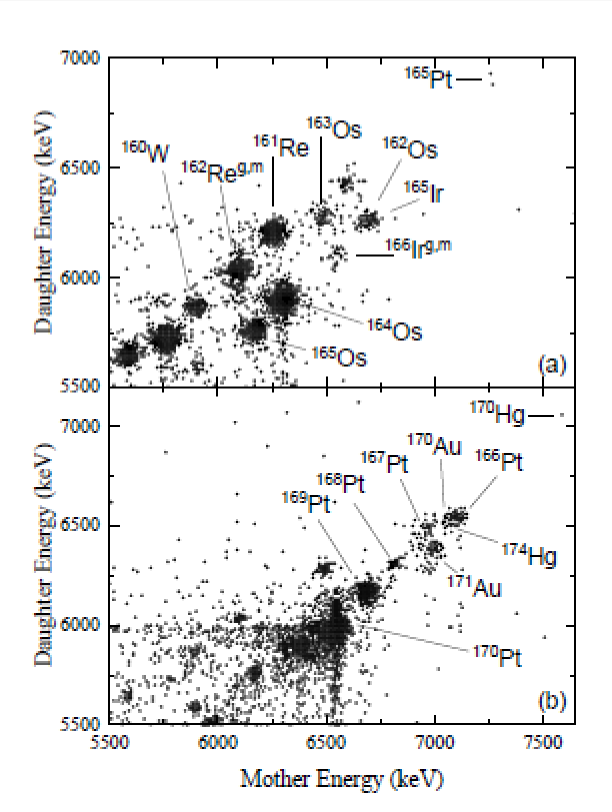

^{160}Os, A. Briscoe et. al., to be publsihed.

APS/123-QED

Alpha spectroscopy studies of ^{166,167}Pt and of the new nuclides ^{165}Pt and ^{170}Hg

J. Hilton,[1,2] J. Uusitalo,[1] J. Sarén,[1] R.D. Page,[2] D.T. Joss,[2] M. AlAqeel,[2] A. Andreyev,[3] H. Badran,[1] A. Briscoe,[2] T. Calverley,[2] D. Cox,[1] T. Grahn,[1] A. Gredley,[2] P.T. Greenlees,[1] R. Harding,[3] A. Herzan,[2] E. Higgins,[2] R. Julin,[1] S. Juutinen,[1] J. Konki,[1] M. Labiche,[4] M. Leino,[1] M. Lewis,[2] J. Pakarinen,[1] P. Papadakis,[1] J. Partanen,[1] P. Rahkila,[1] J. Ojala,[1] P. Ruotsalainen,[1] M. Sandzelius,[1] C. Scholey,[1] J. Sorri,[1] L. Sottili,[1] S. Stolze,[1] and F. Wearing[2]

Charge plunger, talk by J. Heery

NUCLEAR INSTRUMENTS AND METHODS 148 (1978) 369-379 ; © NORTH-HOLLAND PUBLISHING CO.

LIFETIME MEASUREMENTS OF NUCLEAR LEVELS WITH THE CHARGE PLUNGER TECHNIQUE

G. ULFERT, D. HABS, V. METAG and H. J. SPECHT

Physikalisches Institut der Universität Heidelberg and Max-Planck-Institut für Kernphysik, Heidelberg, W. Germany

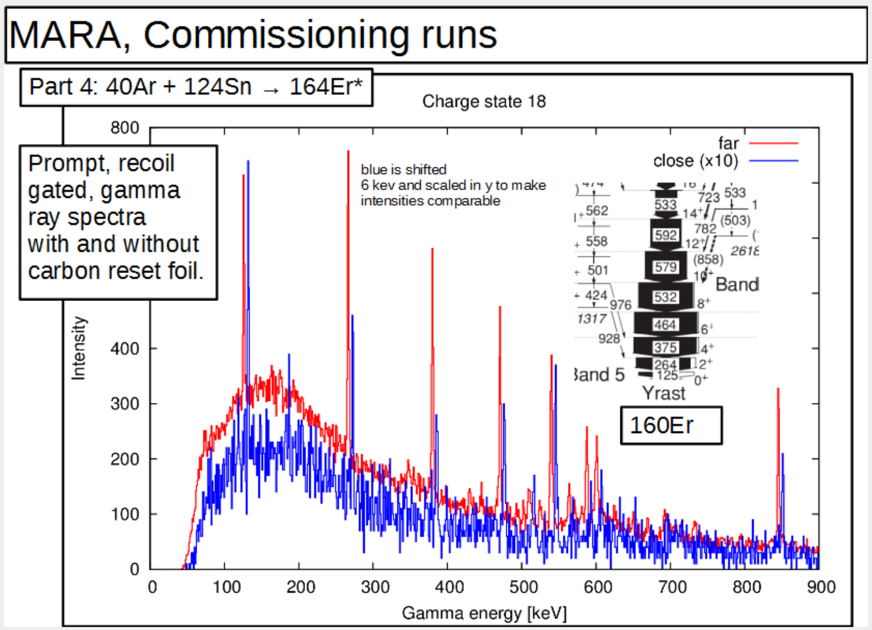

Total conversion is ~1,3 for 125 keV E2, ~ 1ns

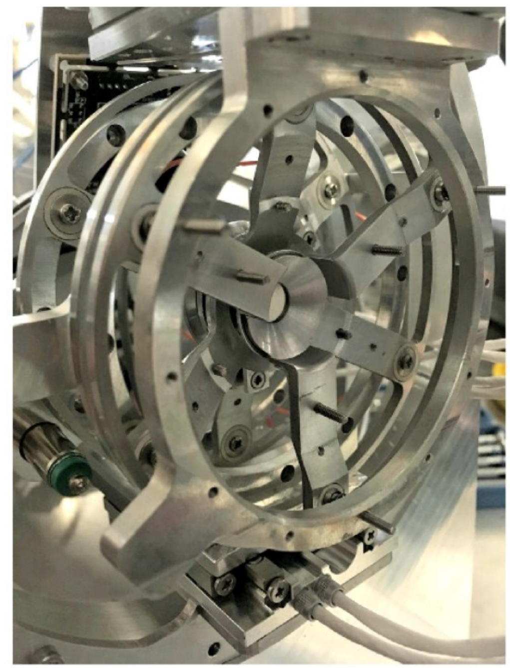

Fig. 7. A photograph of the TPEN. The stopper foil can be seen mounted on a LPS-45 motor on the right of the image. The foil mounts for the degrader and target foils can also be seen.

Recoil shadow method

Z. Physik A 285, 159 – 169 (1978)

Zeitschrift für Physik A

In-Beam Spectroscopy of Low Energy Conversion Electrons with a Recoil Shadow Method – A New Possibility for Subnanosecond Lifetime Measurements

H. Backe, L. Richter, R. Willwater, E. Kankeleit, E. Kuphal*, and Y. Nakayama**
Institut für Kernphysik der TH Darmstadt, Darmstadt, Germany

B. Martin
Max-Planck-Institut für Kernphysik, Heidelberg, Germany

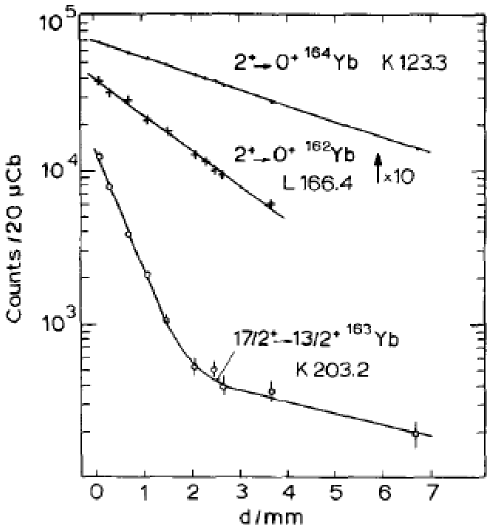

Fig. 12. Life time measurements on certain levels in ^{162,163,164}Yb with the recoil shadow method by variation of the target position d relative to the edge of the semicylindrical baffle. The results are $T_{1/2} = (971 \pm 31)$ ps and $T_{1/2} = (439 \pm 37)$ ps for the $2^+ \to 0^+$ transitions in ^{164}Yb and ^{162}Yb, respectively. For the 203.2 keV transition in ^{163}Yb the two half life components are $T_{1/2}^{(1)} = (108 \pm 7)$ ps and $T_{1/2}^{(2)} = (1.2 \pm 0.3)$ ns

^{208}Pb(^{48}Ca,2n)^{254}No

v = 0.017c = 5.1 mm/ns

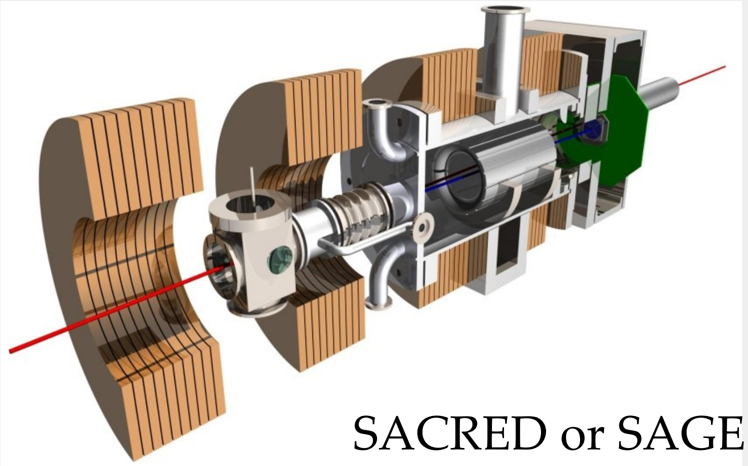

SACRED or SAGE

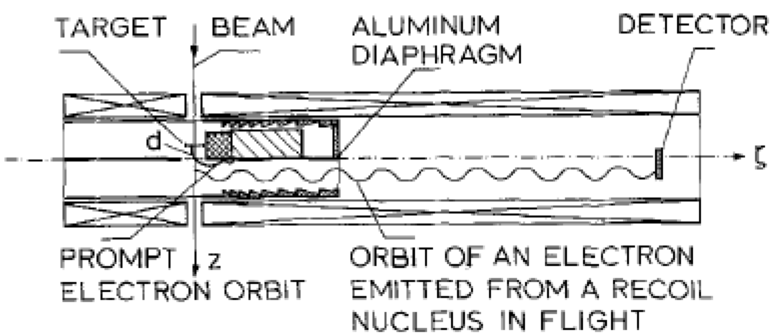

Fig. 8. The recoil shadow method. It is shown a cut through the electron transport system containing the beam and solenoid symmetry axis. The longitudinal baffle avoids detection of prompt electrons but allows very efficiently passage of delayed electrons emitted in flight

Physics Letters B 784 (2018) 199–205

Contents lists available at ScienceDirect

Physics Letters B

www.elsevier.com/locate/physletb

Study of non-fusion products in the $^{50}Ti + {}^{249}Cf$ reaction

A. Di Nitto [a,b], J. Khuyagbaatar [b,c,*], D. Ackermann [b,1], L.-L. Andersson [c,d], E. Badura [b], M. Block [a,b,c], H. Brand [b], I. Conrad [b], D.M. Cox [d], Ch.E. Düllmann [a,b,c], J. Dvorak [c], K. Eberhardt [a,c], P.A. Ellison [e,f], N.E. Esker [e,f], J. Even [a,c,2], C. Fahlander [g], U. Forsberg [g], J.M. Gates [e], P. Golubev [g], O. Gothe [e,f], K.E. Gregorich [e], W. Hartmann [b], R.D. Herzberg [d], F.P. Heßberger [b,c], J. Hoffmann [b], R. Hollinger [b], A. Hübner [b], E. Jäger [b], B. Kindler [b], S. Klein [a], I. Kojouharov [b], J.V. Kratz [a], J. Krier [b], N. Kurz [b], S. Lahiri [h], B. Lommel [b], M. Maiti [h,3], R. Mändl [b], E. Merchán [b], S. Minami [b], A.K. Mistry [d], C. Mokry [a,c], H. Nitsche [e,f], J.P. Omtvedt [i], G.K. Pang [e], D. Renisch [a], D. Rudolph [g], J. Runke [b], L.G. Sarmiento [j,4], M. Schädel [b,k], H. Schaffner [b], B. Schausten [b], A. Semchenkov [i], J. Steiner [b], P. Thörle-Pospiech [a,c], N. Trautmann [a], A. Türler [l,m], J. Uusitalo [n], D. Ward [g], M. Wegrzecki [o], P. Wieczorek [b], N. Wiehl [a], A. Yakushev [b], V. Yakusheva [c]

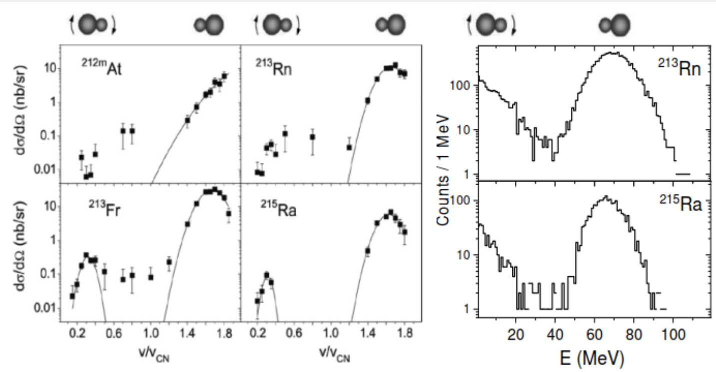

Figure 2. Left panel: The measured velocity (normalized to velocity of CN) distributions of non-fusion products in $^{64}Ni+{}^{207}Pb$ reaction at SHIP (figure is adopted from [26]). To get the cross sections at 10msr forward acceptance angle, the values given in the vertical axis has to be multiplied by a factor 100. Right panel: The measured energy distribution of non-fusion products in $^{50}Ti+{}^{249}Cf$ reactions at TASCA. Illustration of the different orientations as being the origin of the low and high velocity and energy components are given.

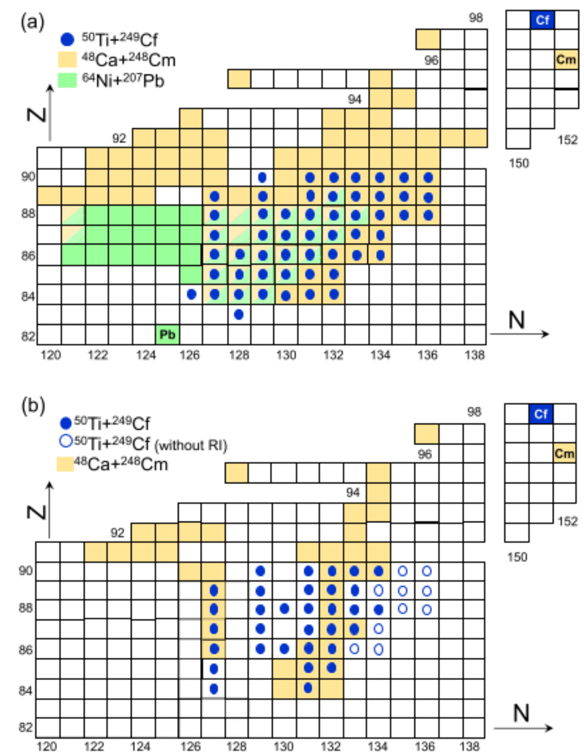

Fig. 3. (Color online.) Cut out of the chart of nuclei in the relevant region [38]. (a) The isotopes identified by their α decay and genetic correlations in $^{50}Ti + {}^{249}Cf$ reactions (blue circles) are compared with those identified in $^{64}Ni + {}^{207}Pb$ [43] and $^{48}Ca + {}^{248}Cm$ [26] reactions marked in green and orange, respectively. (b) Isotopes directly implanted into the focal plane detector. The filled (empty) blue circles correspond to $^{50}Ti + {}^{249}Cf$ reaction products identified in correlation analyses with (without) RI-like events. The orange frames relate to $^{48}Ca + {}^{248}Cm$ reaction products observed in correlation with RI-like events [26,25].

Nuclear reaction dynamics study at MARA

J. Khuyagbaatar[1,2], J. Uusitalo[3], M. Block[1,2,4], Ch. E. Düllmann[1,2,4], R. Herzberg[5], K. Nishio[6], A. Yakushev[2] and the Nuclear Spectroscopy Group[3]

[1]*Helmholtz Institut Mainz, Germany,*
[2]*GSI Helmholtzzentrum für Schwerionenforschung GmbH, Darmstadt, Germany,*
[3]*Department of Physics, University of Jyväskylä, Jyväskylä, Finland,*
[4]*University of Mainz, Mainz, Germany,*
[5]*University of Liverpool, Liverpool, England,*
[6]*Japan Atomic Energy Agency (JAEA), Tokai, Japan*

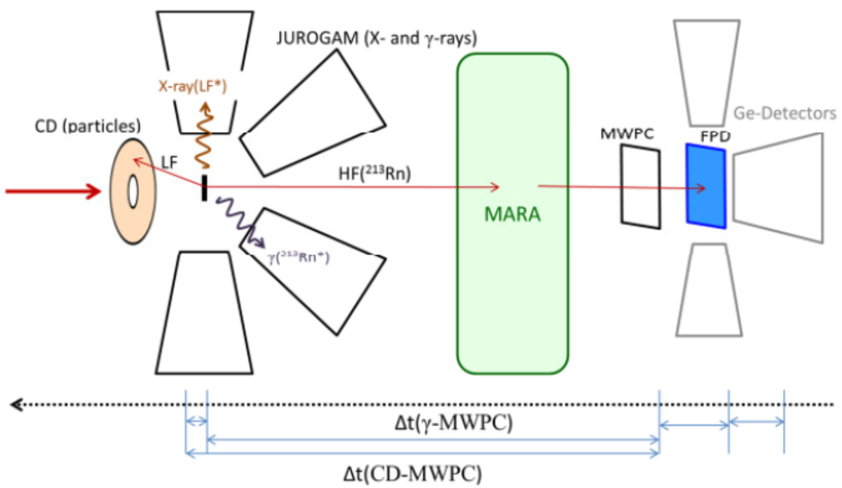

Figure 4. Schematic of the experimental setup and measurement scenario. Notations of the each instrument are given. The horizontal line marks the time scale in a backward direction showing the concept of the delayed coincident technique. See text for details.

^{65}Cu + ^{209}Bi
^{65}Cu + ^{238}U

JUROGAM1 + RITU + GREAT

$^{65}Cu + ^{209}Bi$

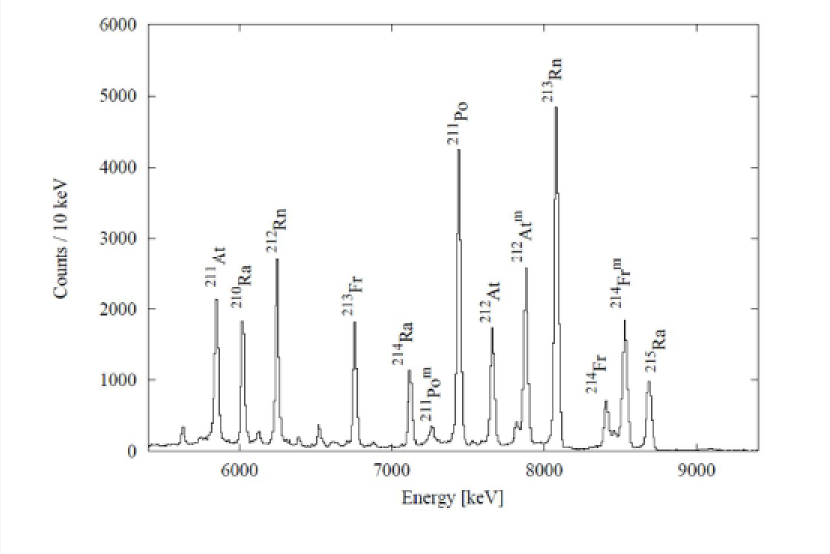

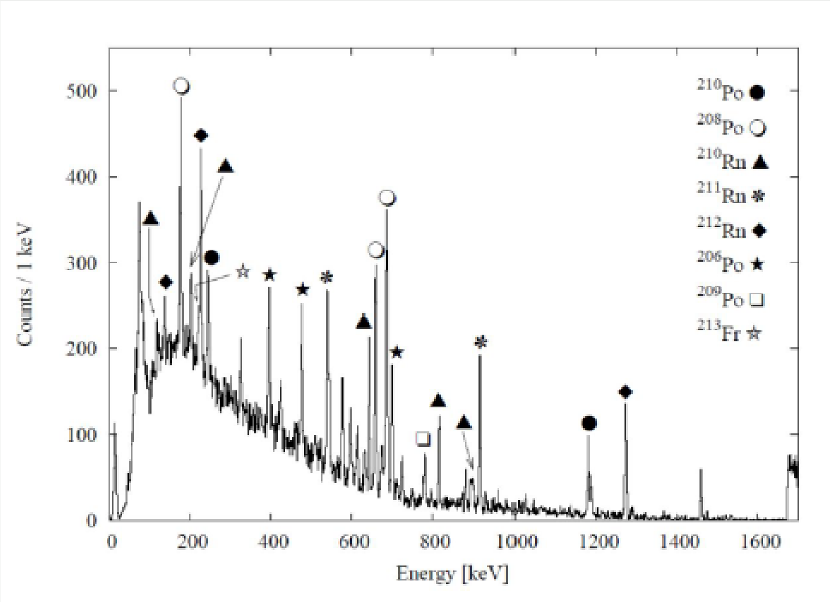

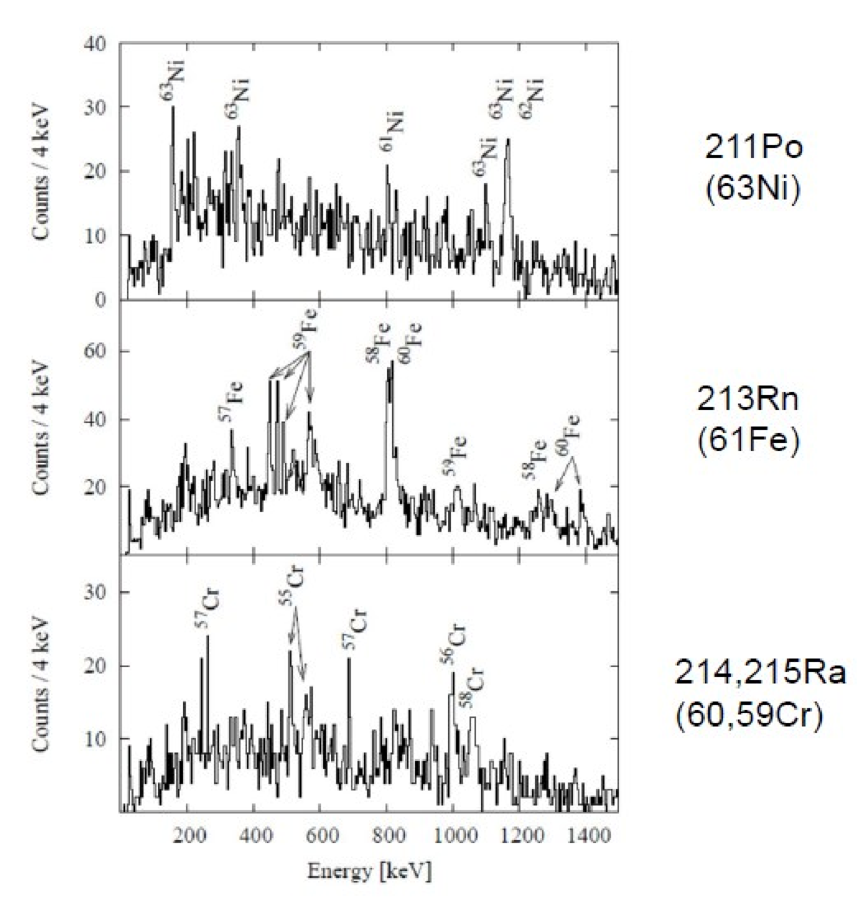

Modification of K130

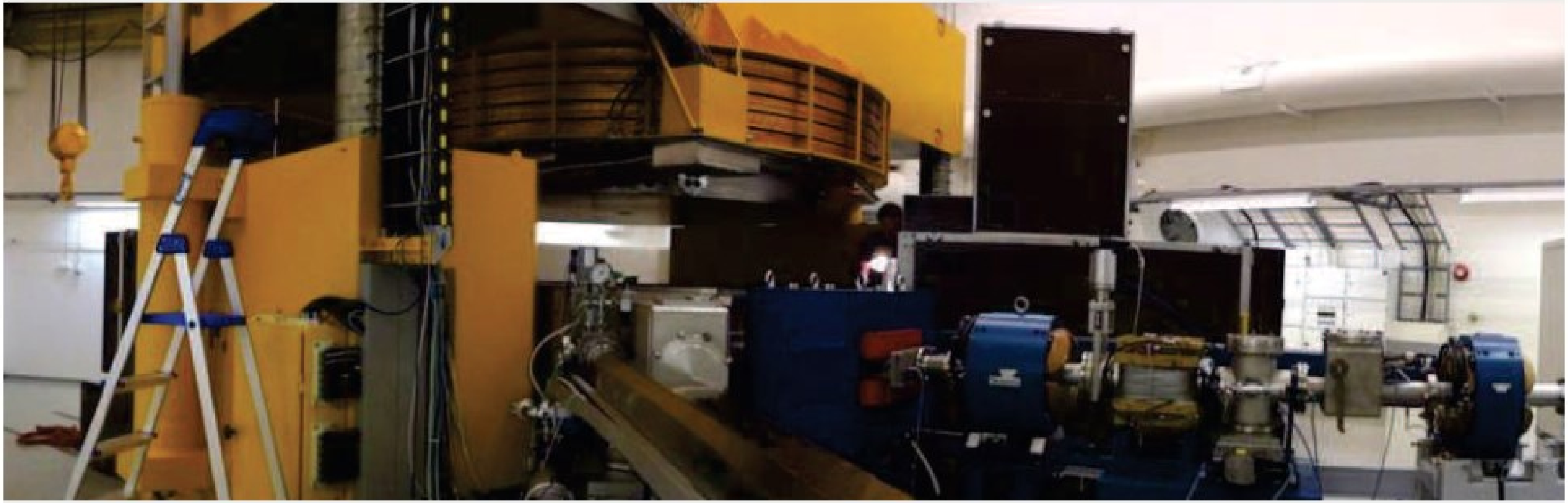

- Higher injection voltage and re-design of cyclotron central region
- Preliminary analysis suggests factor of 8 (x4 transmission, x2 HIISI ECR)
- Will lead to some down time and loss of operations
- Still effectively a single user facility

HIISI 18 GHz ECRIS at JYFL

HIISI specifications:

Strongest PM ECRIS hexapole (1.42 T)

Largest RT ECRIS plasma (0.36 l)

$P_{\mu w}$ (2 x18 GHz) = 4 kW (+ 14.5 GHz klystron). Tested up to 2.4 kW

8-18 GHz TWTA/2 tunable oscillators, not tested yet

Cooled hexapole down to -20˚C: 0˚C presently

Axial field: 2.8T/0.43 T/1.3 T

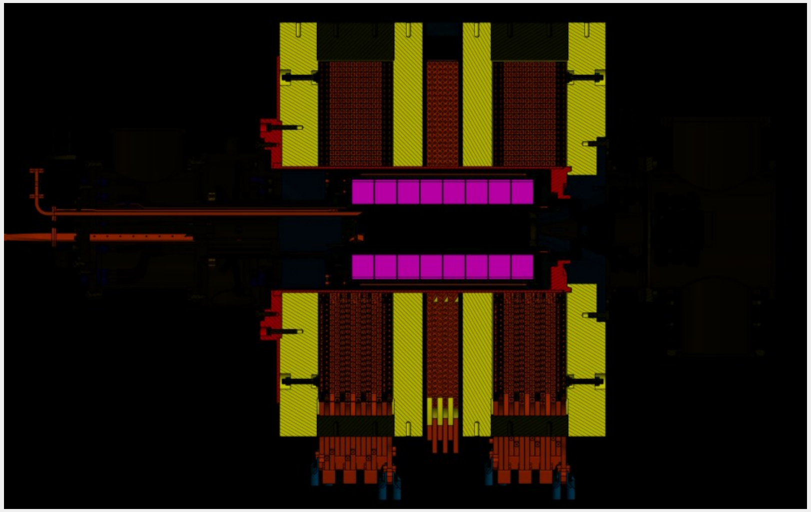

Hannu Koivisto et.al.,

ECR sourses
6.4 GHz
14 GHz

07.02.2019, ^{84}Kr 310 pnA using HIISI, 342 MeV

Results with 36 segment hexapole: argon

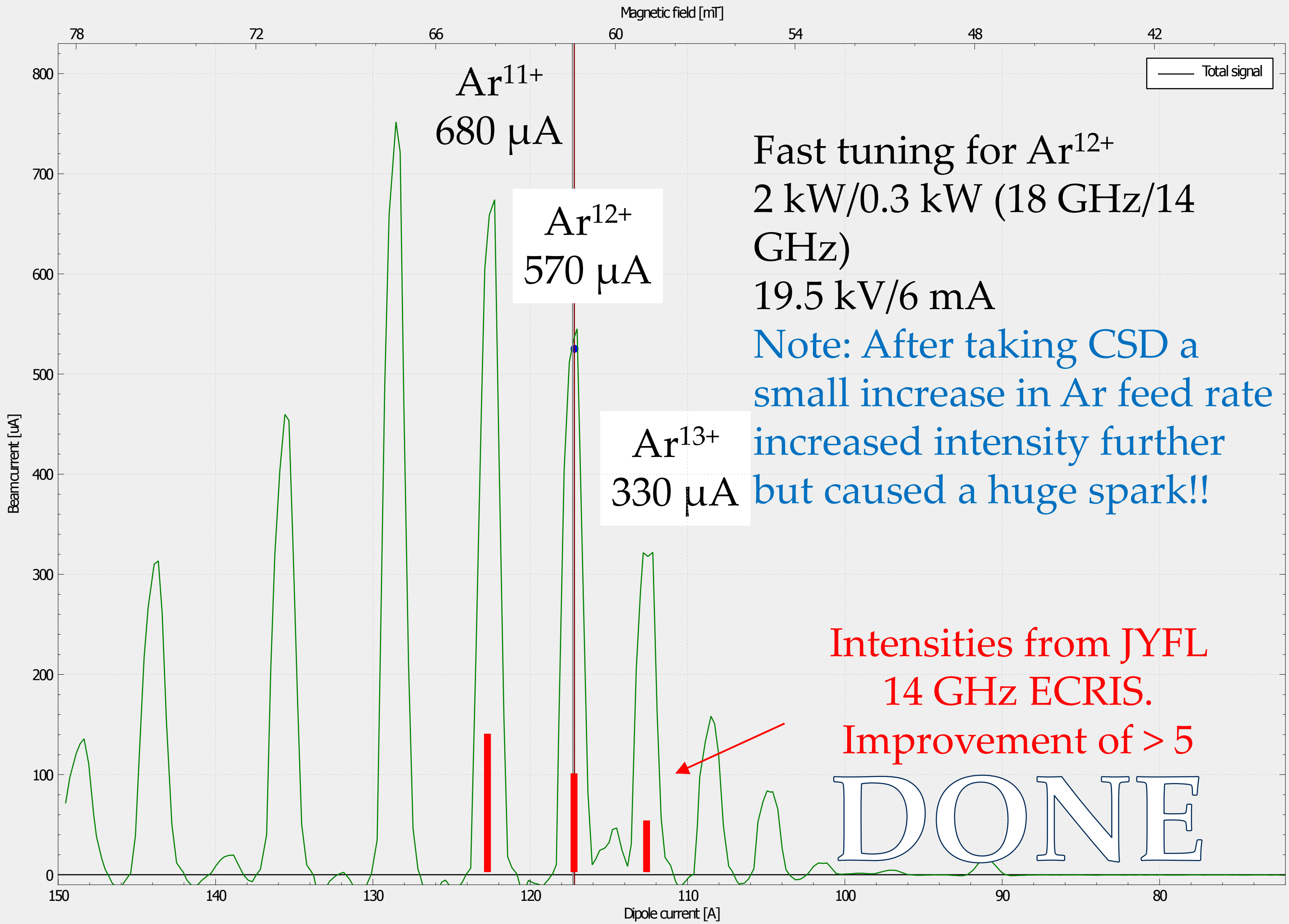

Fast tuning for Ar^{12+}
2 kW/0.3 kW (18 GHz/14 GHz)
19.5 kV/6 mA

Note: After taking CSD a small increase in Ar feed rate increased intensity further but caused a huge spark!!

Intensities from JYFL 14 GHz ECRIS.
Improvement of > 5

DONE

HIGH INTENSITY ION BEAM INJECTION INTO THE 88-INCH CYCLOTRON

D. Wutte[1], D.J. Clark[1], B. Laune[2], M.A. Leitner[1], C.M. Lyneis[1],
[1]Lawrence Berkeley National Laboratory, Berkeley, USA,
[2]Institut de Physique Nucleaire 91406 Orsay Cedex France

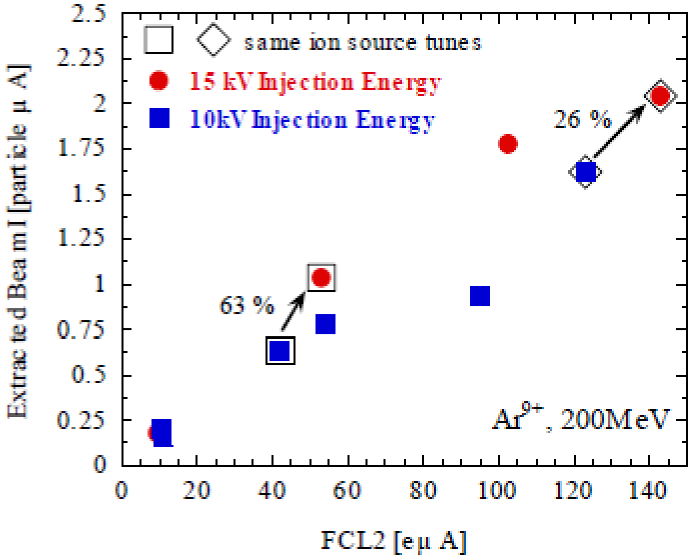

Figure 5: Dependence of the extracted cyclotron current from the analyzed current

K-130 cyclotron,
10 kV injection energy
With high ouptut from the ECR-ion source
1-2 % efficiency
It could be 10-20 %
Plan is to go for 15-20 kV injection energy

Taneli Kalvas

Physics Letters B 764 (2017) 265–270

ELSEVIER

Contents lists available at ScienceDirect

Physics Letters B

www.elsevier.com/locate/physletb

Towards saturation of the electron-capture delayed fission probability: The new isotopes ^{240}Es and ^{236}Bk

J. Konki [a], J. Khuyagbaatar [b,c,*], J. Uusitalo [a], P.T. Greenlees [a], K. Auranen [a,1], H. Badran [a], M. Block [b,c,d], R. Briselet [e], D.M. Cox [f,2], M. Dasgupta [g], A. Di Nitto [c,d], Ch.E. Düllmann [b,c,d], T. Grahn [a], K. Hauschild [h], A. Herzán [a,3], R.-D. Herzberg [f], F.P. Heßberger [c], D.J. Hinde [g], R. Julin [a], S. Juutinen [a], E. Jäger [c], B. Kindler [c], J. Krier [c], M. Leino [a], B. Lommel [c], A. Lopez-Martens [h], D.H. Luong [g], M. Mallaburn [i], K. Nishio [j], J. Pakarinen [a], P. Papadakis [a], J. Partanen [a], P. Peura [a,4], P. Rahkila [a], K. Rezynkina [h], P. Ruotsalainen [a], M. Sandzelius [a], J. Sarén [a], C. Scholey [a], J. Sorri [a], S. Stolze [a], B. Sulignano [e], Ch. Theisen [e], A. Ward [f], A. Yakushev [b,c], V. Yakusheva [b,c]

~ 150 pnA ^{34}S beam for 10 days

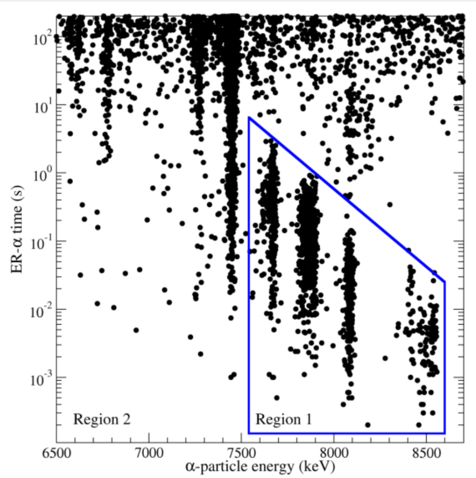

Fig. 2. A two-dimensional plot of the ER–α correlation times on a logarithmic scale as a function of the α-particle energies observed in the ^{34}S + ^{209}Bi reaction. The maximum searching time was 200 s.

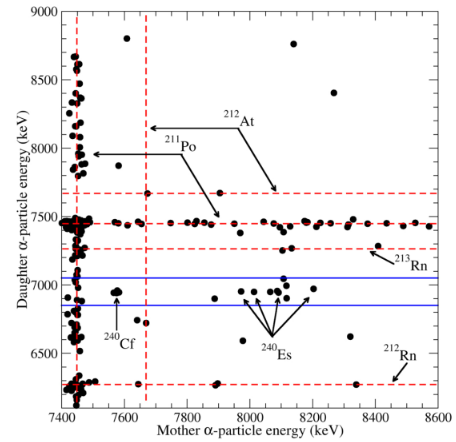

Fig. 4. Mother and daughter α-particle energies for the correlated events of the type ER–α_1–α_2 observed in the ^{34}S + ^{209}Bi reaction. The maximum searching times were 200 s for the ER–α_1 pair and 1200 s for the α_1–α_2 pair. Expected random correlations from the decays of transfer-reaction products are marked with dashed red lines. (For interpretation of the references to colour in this figure legend, the reader is referred to the web version of this article.)

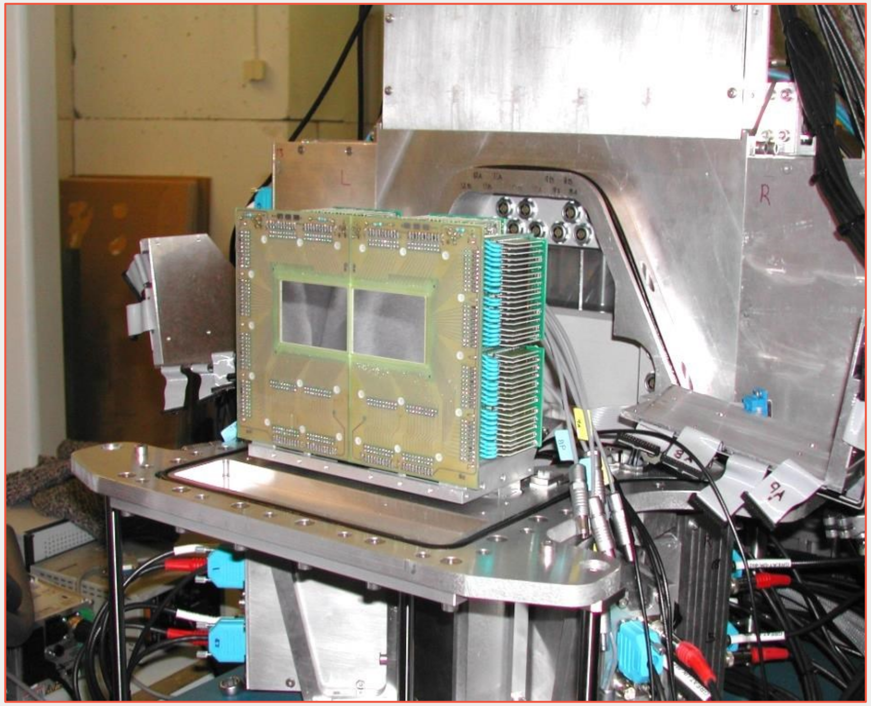

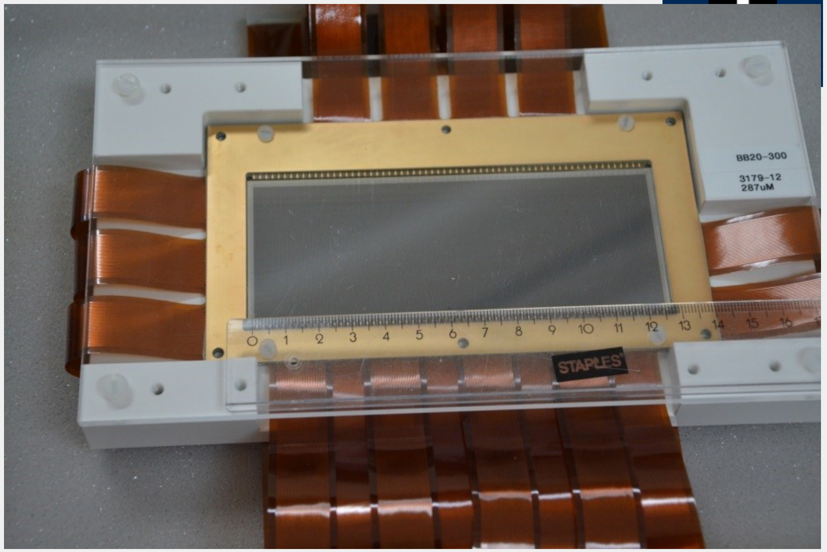

GREAT DSSD 2 x 40 x 60 strips, 200 channels
2 x 40 mm x 60 mm (10 % of strips missing), pixel area 1 mm^2
5-6 mm wide (dead) gap between

MARA DSSD 72 X 192 strips, 264 channels
48 mm x 128 mm (typically ~ 2 strips missing), pixel area 0.45 mm^2

MWPC ugrade 90 % → 94 % transmsission
cathode: foil → wire plane
will help with very low energy recoils

University of Liverpool

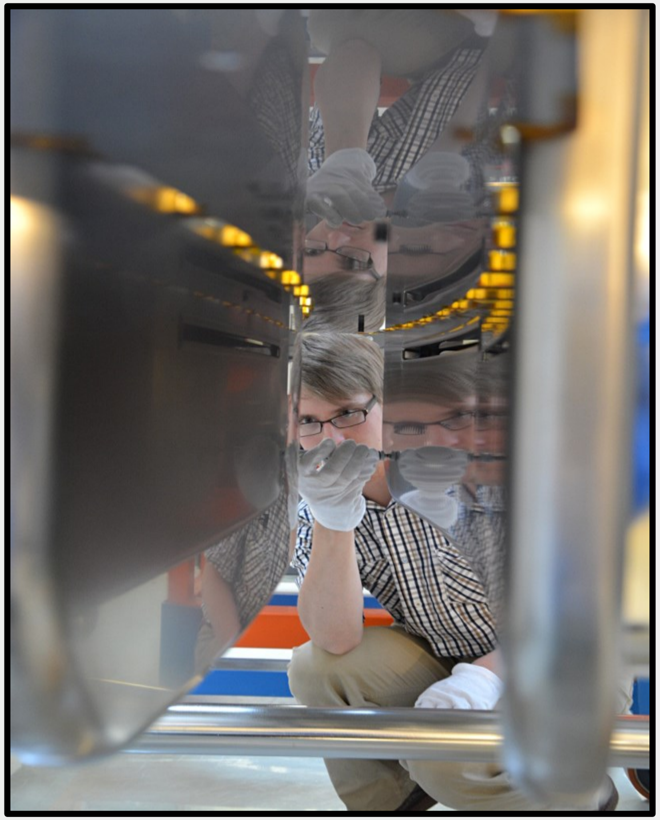

THANK YOU!

Jari Partanen

JU

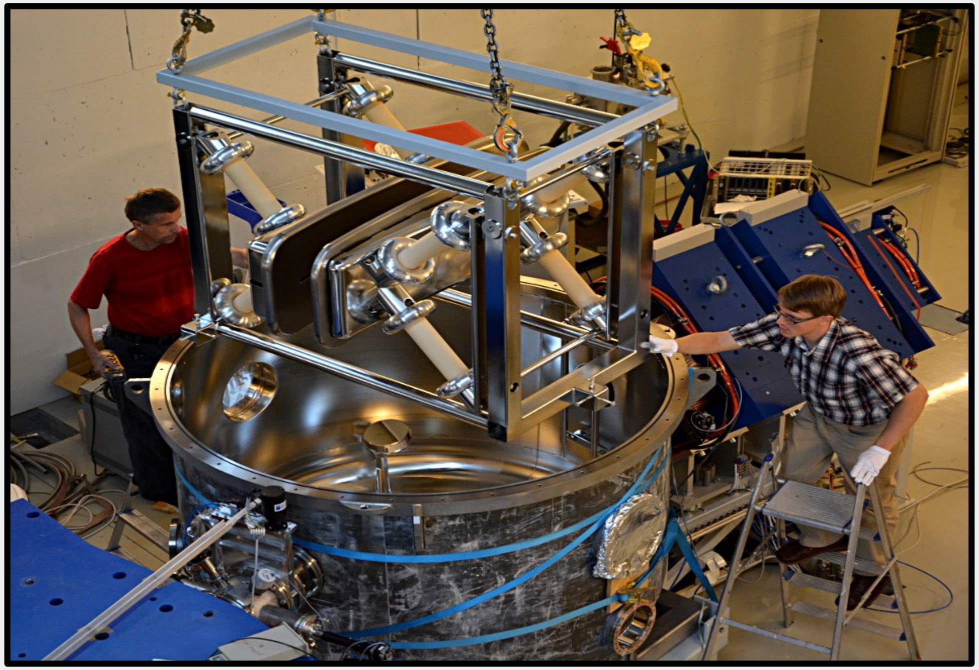

Jan Saren